

**GT2005-68736****THE MEASUREMENT AND PREDICTION OF GASEOUS HYDROCARBON FUEL AUTO-IGNITION DELAY TIME AT REALISTIC GAS TURBINE OPERATING CONDITIONS**

**G-J M Sims, A R Clague, R W Coplestone**  
QinetiQ  
Gas Turbine Technologies  
Farnborough, GU14 OLX, UK  
Tel: +44 (0) 1252 397973  
gjsims@qinetiq.com

**K R Menzies, M A MacQuisten**  
Rolls-Royce plc  
Moor Lane,  
Derby, UK  
Tel: +44 (0) 117 9794596  
Kevin.Menzies@rolls-royce.com

**ABSTRACT**

Auto-ignition delay time measurements have been attempted for a variety of gaseous fuels on a flow rig at gas turbine relevant operating conditions. The residence time of the flow rig test section was approximately 175 ms. A chemical kinetic model has been used in Senkin, one of the applications within the Chemkin package, to predict the auto-ignition delay time measured in the experiment. The model assumes that chemistry is the limiting factor in the prediction and makes no account of the fluid dynamic properties of the experiment.

Auto-ignition delay time events were successfully recorded for ethylene at approximately 16 bar, 850K and at equivalence ratios between 2.6 and 3.3. Methane, natural gas and ethylene ( $0.5 < \phi < 2.5$ ) failed to auto-ignite within the test section. Model predictions were found to agree with the ethylene measurements, although improved qualification of the experimental boundary conditions is required in order to better understand the dependence of auto-ignition delay on the physical characteristics of the flow rig.

The chemical kinetic model used in this study was compared with existing 'low temperature' measurements and correlations for methane and natural gas and was found to be in good agreement.

**KEYWORDS**

Auto-ignition delay time, premix, low NO<sub>x</sub>, gas turbine, flow rig, methane, natural gas, ethylene (ethene).

**INTRODUCTION**

Recent trends in combustor design have been substantially driven by emissions reduction legislation – largely that of oxides of nitrogen (NO<sub>x</sub>). NO<sub>x</sub> emissions are having an increasing impact on local air quality at sea level as well as presenting a continued threat to the upper atmosphere. Compliance with increasingly tough emissions legislation is

therefore critical to the business of gas turbine (GT) manufacturers and operators alike.

Emissions reduction has been technically difficult to achieve, especially those for ultra low NO<sub>x</sub> in land based gas turbine engines. However, in most current applications, reduced emissions are being achieved with the use of lean burn, premixed combustion processes which produce less thermal NO<sub>x</sub> as a result of having relatively low flame temperatures. Unfortunately, one of the inherent disadvantages of premixing fuel and air prior to combustion is exposure to auto-ignition. The onset of auto-ignition can present a major threat to the integrity of the combustion system. Provided that the auto-ignition temperature of the fuel is reached, spontaneous auto-ignition will occur after a characteristic time delay normally referred to as the auto-ignition delay time (ADT). If premix ducts can be designed to achieve adequate mixing in timescales shorter than the characteristic ADT, auto-ignition will be avoided. Thus, the design of a premix duct is heavily reliant upon knowledge of the auto-ignition delay time for a given fuel-air mixture and operating range.

Despite the abundance of methane auto-ignition data available in the public domain, there is currently very little covering the range of operating conditions applicable to industrial and aero-derivative gas turbine engines (<900K). Moreover, the small amount of published data that is relevant to GT application has been found to be conflicting. As a consequence, a flow rig was designed to measure the auto-ignition delay time of gaseous hydrocarbon fuels within a realistic premix duct environment. Measurements made on this rig were used to validate a chemical kinetic model suitable for the low temperature range applicable to GT operation.

This paper presents a combined experimental and modelling investigation into the auto-ignition delay time of natural gas, methane and ethylene fuels at representative GT operating conditions (up to 16 bar and ~900K). The design of a high pressure flow rig, its test configuration and the

accompanying results are discussed in this paper. A brief description of the chemical kinetic model will also be discussed and its low temperature predictive capability will be evaluated against existing correlations and measurements.

## NOMENCLATURE

$\tau$	Auto-ignition delay time (ADT) (ms)
$T$	Pre-ignition air-fuel mixture temperature (K)
$[O_2]$	Concentration of oxygen (mol/cm <sup>3</sup> )
$[CH_4]$	Concentration of methane (mol/cm <sup>3</sup> )
$[HC]$	Concentration of non-methane HC's (mol/cm <sup>3</sup> )
$R$	Universal gas constant (cal/mol-K)
$Tl$	Approximated boundary layer temperature (K)
$\phi$	Equivalence ratio (ER)
$P$	Rig inlet pressure (bar)
$\Delta P_{fuel}$	Fuel driving pressure (bar)

## BACKGROUND

The auto-ignition properties of lower order hydrocarbon fuels have been widely published and, as a consequence, there is an abundance of available ADT data for methane and natural gas mixtures [1 – 17]. However, most of this research has focussed on very high temperatures ( $T > 1400K$ ) – well above gas turbine combustor inlet conditions. As a consequence, a large proportion of these data were obtained using shock tubes – an ideal device to study the chemical kinetics of high temperature methane oxidation [1, 3]. Much of this work was compiled by Spadaccini and Colket [1] in order to derive high temperature correlations for methane and low-order hydrocarbon mixtures given by expressions (1) and (2) respectively:

$$\tau = 2.21 \times 10^{-14} \exp\left(\frac{22659}{T}\right) [O_2]^{1.05} [CH_4]^{0.33} \quad (1)$$

$$\tau = 1.77 \times 10^{-14} \exp\left(\frac{18693}{T}\right) [O_2]^{1.05} [CH_4]^{0.66} [HC]^{-0.39} \quad (2)$$

Their extensive review incorporated published data from an array of shock tubes and flow rig sources and demonstrated that the addition of only a small quantity of higher-order hydrocarbons can dramatically reduce ADT. Due to the popularity of natural gas in the transport and utility industries, there is a large body of literature available which demonstrates the significant impact higher-order hydrocarbon additives have on methane auto-ignition properties. [1, 4 – 8]. However, since most of the experimental data compiled for these correlations were obtained at temperatures above 1400K, neither expression has been validated below ~1300K. Furthermore, the only <1250K sources used in the compilation – obtained from flow rig experiments [9 – 11] – suggest a gross over-prediction in ADT at lower temperatures.

With the increasing importance of methane and natural gas as fuels for internal combustion (IC) and GT engines, studies of ADT at lower temperatures (<1400K) have recently attained greater significance [3, 9 – 17]. Investigations at high pressure and intermediate temperatures (1000 – 1400K) have demonstrated a significant reduction in activation energy below approximately 1300K [12]. From these data, two ADT correlations applicable to the <1300K temperature range have been compiled in the following expressions (3) and (4) [12 & 13] respectively:

$$\tau = 4.99 \times 10^{-14} \exp\left(\frac{19000}{RT}\right) [O_2]^{-1.31} [CH_4]^{0.38} \quad (3)$$

$$\tau = \frac{2.6 \times 10^{-15} [O_2]^{1/3} [CH_4]^{1/3}}{T^{-0.92} \exp(-13180/T)} \quad (4)$$

Compared with the high temperature correlations (1) and (2), the above expressions are in far better agreement with existing flow rig measurements obtained at ~1000K [9 – 11]. However, recent shock tube experiments have demonstrated an additional order of magnitude reduction in ADT when compared with either of the <1300K correlations described above [16, 17]. Significantly however, this work reports several factors which may have adversely affected the results and, as such, raises the question of whether shock tube experiments are suitable for low temperature auto-ignition studies. Consequently, a flow rig was used in this investigation as it was regarded as the most suitable apparatus to study the practical importance of auto-ignition delay time with respect to gas turbine operation. Since ADT is dependent on physical rates such as turbulence, mixing and heat transfer as well as pre-flame chemical kinetics [1], flow rigs can accurately reproduce typical premix duct environments. Moreover, the low temperature range applicable to gas turbine operation is well suited to flow rig apparatus.

The flow rig configuration is briefly discussed in the next section. For a more detailed review of the rig design refer to [18].

## FLOW RIG DESIGN

A photograph and cross-sectional view of the auto-ignition flow rig installation can be seen in Figure 1 and Figure 2 respectively.

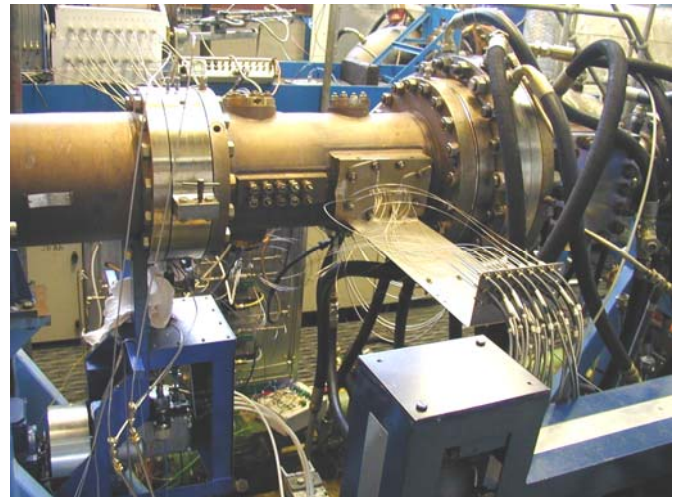


**Figure 1: Photograph of auto-ignition flow rig**

A constant airflow of between 50 and 200 g/s was delivered into the working section of the rig through a venturi flow meter at approximately 16 bar and 900K. The remainder of the airflow – controlled by a perforated plate at the exit of the rig – was allowed to bypass the working section in order to insulate the test duct. Downstream of the venturi flow meter,

the working section consisted of the fuel injector housing and test duct. The fuel injector housing shown in Figure 3 was aerodynamically designed using CFD to prevent the convection of vortices into the test duct which could otherwise support premature auto-ignition. Gaseous fuel was injected into the test duct in 40ms square-wave pulses via a radial fuel distributor designed for rapid mixing. The 0.5m long ( $\varnothing$  0.05m) test duct was aligned with an axial array of wall-mounted fibre optic sensors used to detect the onset of auto-ignition.

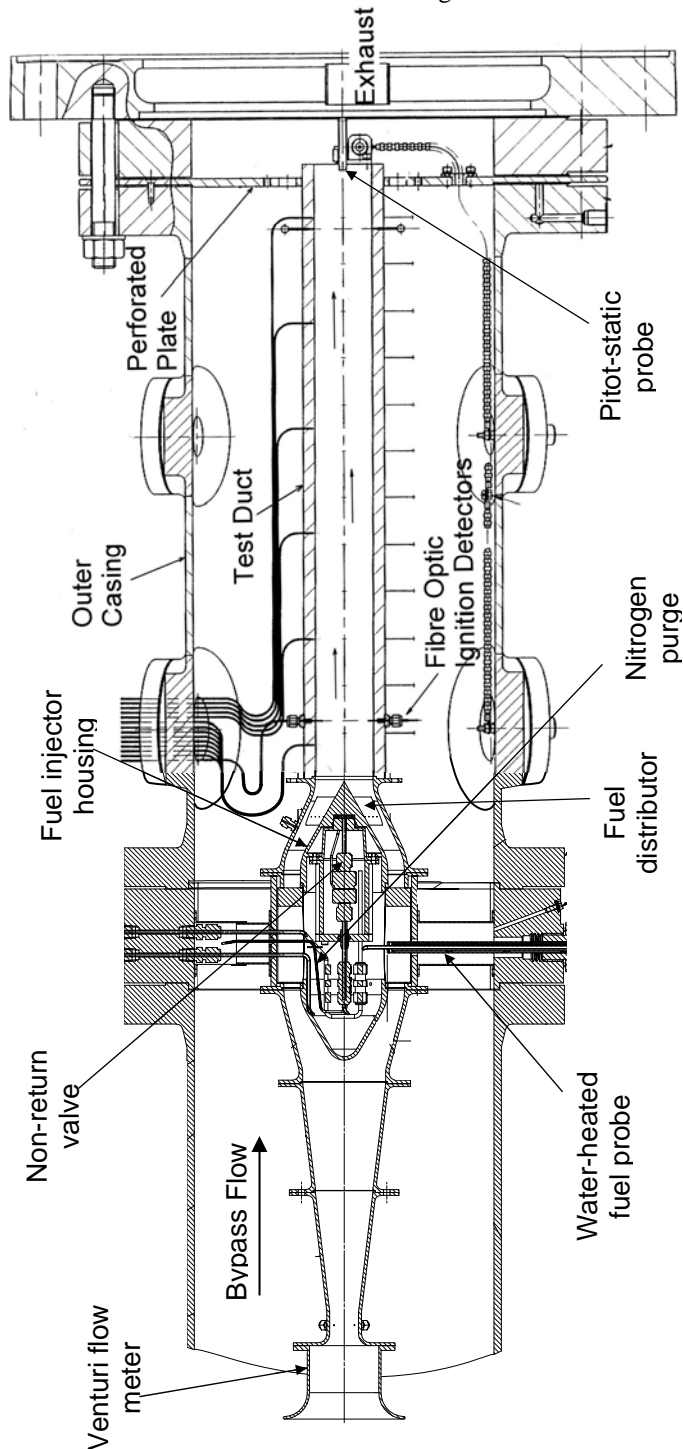


Figure 2: Cross-sectional view of auto-ignition flow rig

## PULSED FUEL INJECTION SYSTEM

A schematic of the fuel injection system is given in Figure 4. A pulsed system was employed to minimise the risk of flashback, thermal loading and over-pressurisation due to high pressure ignition. Preventing flashback was particularly important as the bulk mixture velocities were of the same order as the turbulent flame speed.

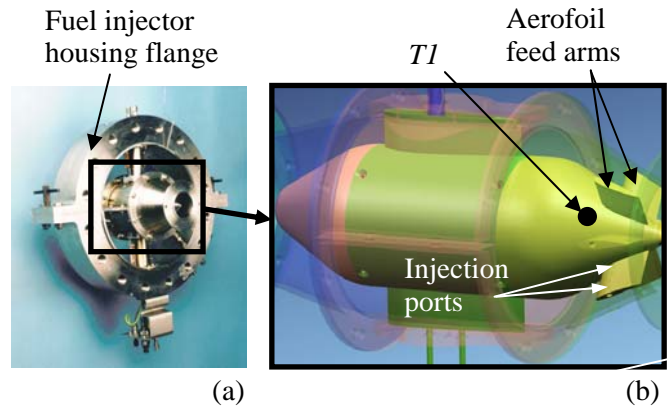


Figure 3(a): Outer wall and flange of fuel injector housing; (b) Fuel injector housing (transparent view of outer wall)

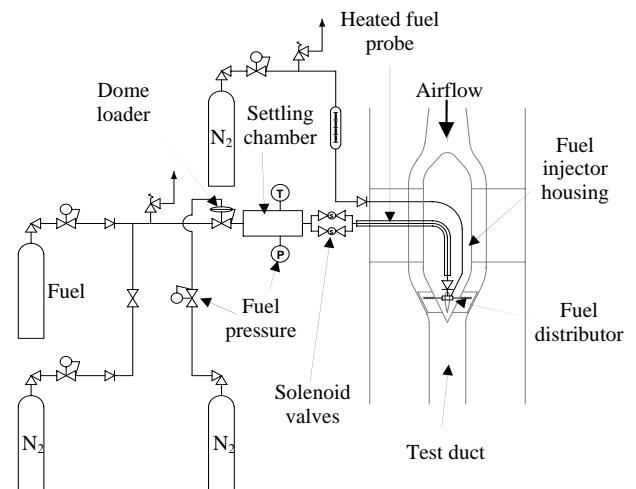


Figure 4: Fuel injection system schematic

High pressure gaseous fuel was stored in a heated settling chamber upstream of two fast-acting Peter Paul H22H7DGV solenoid control valves. The valves were controlled by duplicate high-speed solenoid valve drivers with a common drive signal that was logged at a rate of 5000Hz. The downstream fuel pressure was controlled with a nitrogen-charged dome loader and a pulsed flow number was characterised across a range of driving pressures and pulse widths using a high-pressure fuel injector calibration rig. Since the solenoid valves were located outside of the pressure casing, the calibration rig was also used to determine the time delay between the control signal and the point of fuel injection. The impact of fuel compressibility and purge/prime transients on pulse shape were also characterised in detail on the same rig [18]. Figure 5 gives an example of the pressure response of a



40ms fuel pulse in relation to the valve drive signal. Pulsed flow number and purge/prime characteristics were found to be constant above 40 ms, thus establishing the minimum required pulse length for the test campaign.

As a further consequence of employing an external fuel control system, a continuous nitrogen purge and non-return valve were installed to prevent diffusion of hot air into the fuel line (and thus to avoid premature auto-ignition and/or flashback).

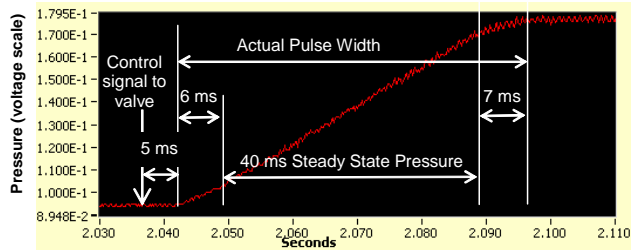


**Figure 5: Pressure response of 40 ms pulse at  $\Delta P_{fuel} = 31$  bar**

A water-heated fuel probe was used to maintain a constant fuel inlet temperature of  $100^{\circ}\text{C}$  – the maximum operating limit of the solenoid valves. Thus the fuel injector housing was designed to remove as little heat as possible from the outer wall of the fuel injector housing to prevent cool boundary layer formation. However, as a precaution, a thermocouple,  $T1$ , was located 1.0 mm from the outer wall of the fuel injector housing to provide an indication of the boundary layer temperature immediately upstream of the fuel entry point (see Figure 3(b)).

#### FUEL DISTRIBUTOR DESIGN

A high-pressure drop, aerodynamic radial fuel distributor was designed to optimise fuel-air mixing at entry into the test duct. It consisted of a central fuel gallery surrounded by six radial aerofoil feed arms. The central gallery incorporates an array of 60 pedestals ( $L/D = 3:1$ ) to augment fuel surface contact with the hot section of the housing unit in order to maximise fuel injection temperature. Each fuel feed arm was manufactured to a NACA 0021 standard aerofoil profile in order to minimise the level of turbulence being convected into the test duct. Radial distribution was achieved by introducing fuel through  $\text{Ø}0.5 \text{ mm} \pm 0.1\text{mm}$  fuel injection ports at four separate radial locations on each side of the aerofoil. The injection ports were designed to choke across the full range of equivalence ratios and located to ensure plug flow and adequate mixing across the full diameter of the duct.

In order to maximise test duct residence time by minimising air massflow, the free stream turbulence levels in this experiment were lower than would otherwise be expected in a typical premix duct. As such, the test rig was heavily reliant upon rapid fuel-air mixing at the fuel distributor in order to obtain a uniform equivalence ratio across the test duct. Consequently, the fuel-air mixing characteristics along the test duct were analysed using CFD.

#### FLOW RIG MODELLING

A CFD model was constructed of the auto-ignition rig, as shown in Figure 6. The model includes the venturi inlet duct, fuel injector housing and distributor (centrebody) and downstream test duct. The complete geometry was modelled to avoid any assumptions on symmetry in the flow.

A structured non-orthogonal grid was used for the calculations, comprising over 400,000 cells for the domain. The governing Favre-averaged Navier-Stokes equations were employed along with a low Mach number assumption, so that density variations arise from mixing alone. Turbulence was modelled using the standard  $k-\epsilon$  model with wall functions to represent the semi-viscous near wall region. The governing equations were discretised on a colocated cell-centred grid, with the Rhie and Chow [19] procedure employed to prevent pressure-velocity decoupling. The calculations used a non-diffusive and bounded scheme for convection [20] to permit resolution of steep gradients while not introducing unphysical oscillations.

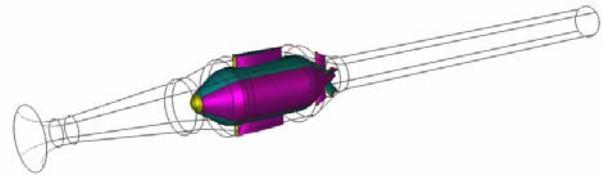


**Figure 6: CFD model domain**

The computational results are presented as circumferentially averaged profiles of air-fuel ratio (AFR) along the duct. Results are presented for two cases:  $\phi = 0.5$  (lean) and  $\phi = 1.2$  (rich). Profiles are plotted at various axial distances downstream of the fuel injection locations to show the mixing development.

Figure 7 shows the mixing development along the test duct for both the lean and rich cases. In general, it can be seen in both cases that as the fuel-air mixture is convected along the duct, the AFR profile becomes more uniform as the fuel mixes into the air stream. The higher momentum produced in the rich case results in greater turbulence and penetration and thus leads to better mixing at all stations. Mixing is not completely uniform however, since in both cases more of the fuel tends to be concentrated in the near-wall region and fails to fully mix further downstream. Nevertheless, the increase in AFR immediately adjacent to test duct wall suggests that not all of this additional fuel penetrates into the boundary layer. This is particularly true of the first station ( $dx = 0.05$ ) and in the lean case, where fuel jet momentum is low and not able to penetrate far into the near-wall region. Once again however, fuel concentration gradients in this region are less apparent in the rich case where mixing throughout the test duct is generally improved.

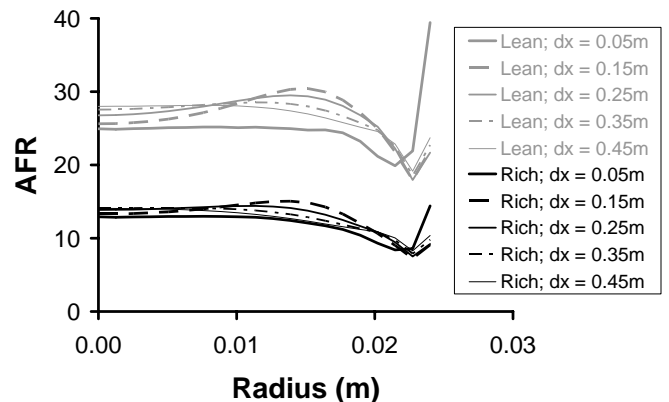


**Figure 7: Mixing development for lean & rich cases**

## EXPERIMENTAL CONFIGURATION

### FUEL

Table 1 provides a list of all fuels used in the experiment. The composition of natural gas was based on the German Ruhr gas field supply.

	Methane	Natural gas	Ethylene
Methane, CH <sub>4</sub>	>99.9%	85.5%	-
Ethylene, C <sub>2</sub> H <sub>4</sub>	-	-	>99.9%
Ethane, C <sub>2</sub> H <sub>6</sub>	-	3.1%	-
Propane, C <sub>3</sub> H <sub>8</sub>	-	0.6%	-
n-butane, C <sub>4</sub> H <sub>10</sub>	-	0.1%	-
Nitrogen, N <sub>2</sub>	-	9.2%	-
Carbon dioxide, CO <sub>2</sub>	-	1.5%	-

**Table 1: Fuel composition**

### INSTRUMENTATION

An average venturi inlet static air pressure was measured from four circumferentially aligned tappings ganged to a pizo ring using a 20 bar pressure transducer. This pressure line was also routed to the +ve side of a 140 mbar differential pressure transducer. The -ve side of the transducer was coupled to an average venturi throat static pressure measurement once again taken from four tappings ganged to a second pizo ring. Two venturi inlet temperatures were measured immediately downstream of the entry bellmouth at top and bottom dead centre.

Nineteen Ø200 µm high temperature fused silica fibre-optics with a nominal ±14° field of view were used to measure full bandwidth light emitted from within the test duct at the point of ignition.

Test duct velocity was computed from the total pressure at duct exit, which was measured using a 1/16" pitot tube mounted on the duct centreline. The pitot tube was connected to the +ve side of a 20 mbar differential pressure transducer, whereas the -ve side measured the duct exit static pressure. Both pressure lines were balanced to avoid over-pressurisation upon the point of ignition.

Four Ø1 mm k-type thermocouples were used to record the axial metal temperature gradient across the test duct. A similar thermocouple was used to measure the approximated fuel injector housing boundary layer temperature,  $T_l$ .

The fuel inlet temperature was maintained at 100°C using insulated heated tape. The heated tape temperature was controlled using a dipped thermocouple installed inside of the fuel settling chamber.

The temperature of the water flowing both out of the non-return valve water jacket and also into and out of the fuel probe were monitored using dipped thermocouples. Heated water flow rates were maximised to maintain a constant 100°C circuit temperature.

### HIGH SPEED DATA ACQUISITION

The twin-solenoid control valve drive signal and all 19 fibre-optic responses were simultaneously recorded and analysed using a LabVIEW-based data acquisition system logging at a rate of 5000 Hz. LabVIEW Version 5.1 was used in conjunction with an SCXI 1140 sample and hold board (National Instruments).

The data acquisition system (and fibre-optics) were commissioned prior to the auto-ignition tests by applying a 10 Hz blue LED to each channel (10 volts, 50 ms pulse width). The corresponding voltage signals were recorded and analysed at 5 kHz and no discrepancies were found.

### OPERATING RANGE

The 5.8 MW inter-cooled heat exchanger used on QinetiQ's high pressure test bed required an airflow of approximately 3 kg/s at 16 bar to achieve an output air temperature of 900K. At this condition, approximately 60% of the air was removed upstream of the rig and of the remaining flow, about 90% was bypassed around the working section. Depending on the balance of these flows, venturi inlet temperatures varied between 867K and 887K. More importantly, the heat loss along the working section varied as a function of both test duct and bypass air velocity. For gaseous operation, the rig was designed to operate with test duct velocities between 4 and 16 m/s, giving a test duct bulk flow residence time of between 120 and 30 ms. Corresponding bypass air velocities varied from 2 to 5 m/s respectively. The large turndown in air velocity – particularly inside the working section – was found to have a significant effect on the approximated 'boundary layer' temperature,  $T_l$ , which varied from 847K to 881K. The temperature loss along the test duct however, remained at approximately 10°C irrespective of airflow rate.

Figure 8 gives the operating limits of the test rig at 16 bar. It is important to note that the rig operating boundary satisfies the ADT range of interest since delay times greater than ~100ms will have very little impact on GT applications as premix duct mixing times are typically an order of magnitude lower.

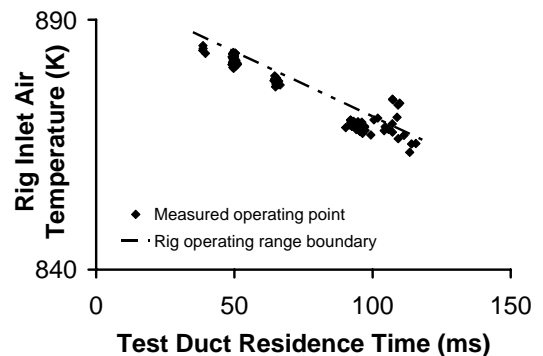


**Figure 8: Operating limits of test rig at 16 bar**

Depending on test requirements, adjustment of the bleed flow split enabled the rig to achieve maximum air temperature or maximum test duct residence time. Furthermore, since CFD had shown a non-uniform fuel distribution near to the duct wall, the influence of fuel-air mixing could be studied by varying the duct velocity and hence free-stream turbulence levels.

## RESULTS & DISCUSSION

### METHANE & NATURAL GAS

For every test point attempted, between 10 and 20 pulses of fuel were supplied to the test duct in time intervals of between 1 and 5 seconds. This was done to obtain a good

statistical sample at a fixed operating point. With a time period of 1 second or less, it was found that the nitrogen purge always remained isolated from the fuel distributor since it took about 1 second for all of the fuel to be purged after each pulse. In doing so, the interaction between the hot air and the temporarily stagnant fuel after a number of pulses eventually caused an auto-ignition event immediately downstream of the fuel distributor. Although the rig was not designed to operate in this manner – since it exposed it to the possibility of flashback – this exercise yielded valuable information on the comparative readiness of methane and natural gas to auto-ignite. It was found that across the full equivalence range, natural gas consistently ignited after a fewer number of pulses in comparison to methane, thus providing quantitative evidence that natural gas has a quicker auto-ignition delay time than methane at the test conditions observed.

Consequently, only natural gas measurements were attempted across the full operating range given in Figure 8 with equivalence ratios ranging from 0.5 to 3.3 (although the rich limit was only achievable at the maximum residence time condition). Methane measurements were attempted, but only at a limited number of test points and operating conditions [bulk flow residence time ~70ms; air inlet temperature ~855K; equivalence ratio between 1.3 and 1.9]. Up to 20 pulses were injected into the test duct in 5 second time intervals for every attempted measurement point and on no occasion was a measurable auto-ignition event observed for either fuel. The auto-ignition delay time of natural gas was thus demonstrated to be greater than the measured test duct residence time (~120 ms) at the cited conditions and for this particular experimental configuration.

Since it was not possible to obtain ADT flow rig data using methane or natural gas, ethylene was selected as a potential validation fuel for the chemical kinetic model. Ethylene was chosen as a consequence of its high volatility and applicability to the model [21].

## ETHYLENE

Successful auto-ignition events were recorded with ethylene at  $15.85 \pm 0.02$  bar;  $870 \pm 2$ K inlet air temperature;  $TI = 848 \pm 2$ K and at mean equivalence ratios between 1.6 – 3.5  $\pm$  0.1. Measurements were also attempted across a range of leaner (down to 0.6) and higher temperature/lower residence time conditions, although without success.

ADT was measured using the following two techniques:

1. Divide the distance to the first detected light signal by the test duct centreline velocity.
2. Measure the time delay between the control valve and the first detected light signal. The time delay between the control valve and fuel entry into the test (measured during the calibration of the fuel injection system) was then subtracted to give ADT.

The latter technique was only considered valid if the duration of the light signal was equal to, or greater than the pulse width (i.e. ignition occurred at the leading edge of the fuel ‘slug’).

Table 2 gives the measured ADT values obtained for both techniques with respect to equivalence ratio. Fewer measurements were obtained using the second method since the auto-ignition events occurring towards the leaner end were registered for less than the pulse width. It is also clearly evident

that the two techniques give two very different data sets; the second yielding ADT values approximately 60 ms longer than the first. Upon closer inspection it was found that the auto-ignition events were taking place near the wall boundary where mixture propagation velocities were much lower than the bulk flow. As a consequence, evidence of partial flashback was observed in some instances, although the detected light signal was weak and disappeared long before it reached the fuel distributor. The first measurement technique was thus considered invalid since it relied exclusively upon the bulk flow velocity. In contrast, knowledge of the velocity flow field was not required for the second method and was consequently found to be a more robust approach. Nevertheless, a level of uncertainty must be attributed to both the local equivalence ratio and mixture temperature in light of the near-wall fuel distribution gradient as shown by CFD. Moreover, the impact of free-stream turbulence on fuel-air mixing could not be investigated since auto-ignition was only observed at one specific temperature – residence time operating point.

Inlet pressure, bar	Inlet temperature, K	TI, K	$\phi$	ADT 1, ms	ADT 2, ms
15.84	867	845	1.6	99	-
15.86	867	846	1.6	97	-
15.86	868	846	1.6	94	-
15.83	868	845	1.6	93	-
15.87	868	845	2.1	90	-
15.87	869	846	2.1	91	-
15.86	869	847	2.1	93	-
15.85	869	846	2.2	93	-
15.85	868	846	2.1	81	-
15.83	868	846	2.6	88	-
15.83	869	847	2.5	86	159
15.86	869	847	2.5	95	-
15.86	868	846	2.5	88	151
15.83	869	847	2.5	94	-
15.84	869	846	2.4	84	148
15.86	868	846	2.5	93	-
15.85	869	848	2.5	86	148
15.83	869	847	2.9	82	-
15.83	869	850	2.8	86	137
15.86	869	847	2.9	82	-
15.85	869	846	3.0	86	141
15.84	870	847	2.9	83	147
15.85	869	846	3.0	86	-
15.84	869	847	2.9	86	154
15.84	869	847	2.9	89	-
15.85	870	847	2.9	85	153
15.87	870	848	3.5	73	-
15.87	869	850	3.5	86	136
15.83	870	848	3.6	81	-
15.83	870	848	3.4	68	127

**Table 2: Ethylene ADT measurements**

In summary, ethylene was proven to have a shorter auto-ignition delay time compared to methane and natural gas at the given test conditions. In the context of GT operational integrity therefore, an ADT in excess of ~150 ms cannot be considered a major risk since GTs generally rely on far shorter premix duct mixing times.

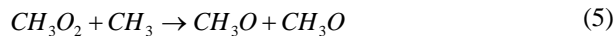
## MODELLING

The results of the experimental test programme were compared with those of a chemical kinetic model designed to simulate the auto-ignition chemistry of a gas mixture. The purpose of the model was to investigate the chemical delay

time and so no allowance was made of the physical processes such as mixing and boundary layer phenomena.

In compiling the kinetic model, it was important to use a chemical mechanism that had been validated at the low temperatures at which ignition events were attempted. A number of previous modelling studies had used the well-known GRI mechanism for methane combustion [22], but this has only been validated to ~1200 K, well above the temperatures found within the experimental duct. Instead, the mechanism of Konnov [21] was used, which contains lower temperature chemistry that has been validated by the author to temperatures down to at least 900 K [23].

The Konnov reaction scheme contains over 120 chemical species and over 1000 reversible chemical reactions, many of which are specifically aimed at low temperature combustion. For example, Petersen [12] cites the reaction between the methyl and methyl peroxy radicals as being among those key to controlling ignition phenomena at 1100K:



The species  $CH_3O_2$  and its relevant reactions are all included in the Konnov mechanism used in the current modelling study, but not in the GRI mechanism.

Another advantage of the Konnov mechanism over the GRI mechanism with regard to the current work is that it was designed for small hydrogen combustion, which allows for the use of both  $C_2$  and  $C_3$  hydrocarbons as primary reactants. While the GRI mechanism is capable of modelling methane and natural gas combustion, it is not suitable for modelling ethylene as a pure fuel.

The chosen kinetic mechanism was used in conjunction with the Senkin program from the Chemkin package [24]. The flow within the test duct was modelled as a homogeneously reacting gas mixture under constant pressure, adiabatic conditions. Ignition was then adjudged to have occurred once the mixture temperature had risen by 400 K. The gases were assumed to be perfectly mixed and that the fuel attained the same temperature as the airflow instantaneously.

### ETHYLENE PREDICTION

The initial model boundary conditions of temperature, pressure and reactant concentrations were taken from Table 2. Since the experiment had demonstrated auto-ignition within the boundary layer,  $T_I$  was used as it was adjudged to be the best indication of the near-wall temperature inside the test duct.

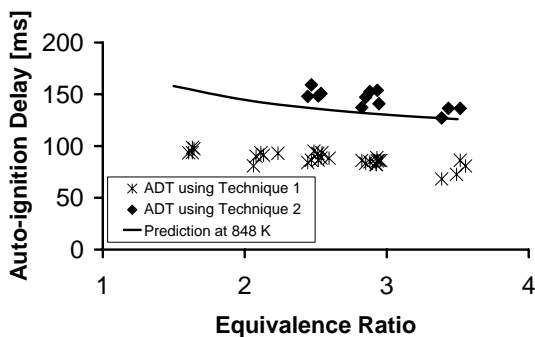


Figure 9: Comparison of ethylene ADT measurements and model prediction at 848K

Figure 9 shows good agreement between the experimental and predicted auto-ignition delay time as a function of mean equivalence ratio. Interestingly, the ADT was found to decrease with increasing fuel addition in both cases.

Assuming the chemical model is valid at ~850K, the close match between the two sets of results either suggest that the physical processes have a negligible effect on ADT or that the model boundary conditions are poorly defined. Improved characterisation of the near-wall boundary conditions together with a better spatial understanding of where the auto-ignition event occurred within the test duct should help eliminate this uncertainty.

### METHANE PREDICTION

Given the good agreement between the model and the experimental results for ethylene, the kinetic model was compared with published methane data at 10 atm and  $\phi = 0.5$  in Figure 10. Measurements from flow rig [9 – 11] and shock tube [16, 17] experiments are used, although there are no available data at operating conditions applicable to this study. As a consequence, low temperature correlations (3) and (4) are included to predict ADT values at typical gas turbine operating conditions. Figure 10 also includes predictions from GRI-Mech Version 3 (GRIM3) [22]. GRIM3 is the latest chemical kinetic reaction scheme for methane combustion, although is only valid for temperatures above 1350K.

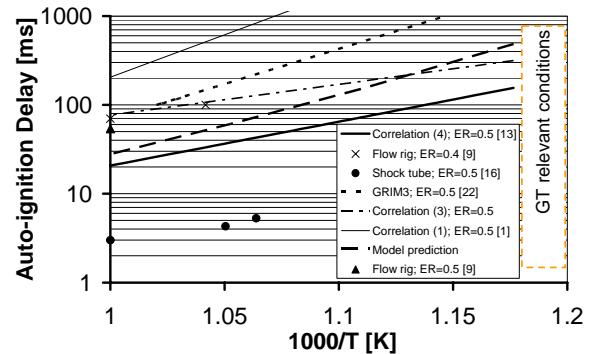


Figure 10: Comparison of published methane ADT data with model prediction at 10 atm and  $\phi \sim 0.5$

Firstly, the order of magnitude difference between the shock tube measurements and all other existing data may allude to the experimental uncertainty of this measurement technique at low temperatures. Incident shock pre-heating, boundary layer formation, inconsistency of diaphragm rupturing and physical geometry limitations may all contribute to the difficulties associated with shock tube measurements at low temperature [16, 17].

In contrast, correlation (1) arguably over-predicts ADT even at 1000K, and thereafter notably diverges from all other sources of data as temperature decreases. This is not surprising however, since the expression was derived almost exclusively from high temperature data [1]. Likewise, GRIM3 exhibits a similar, albeit less severe divergent trend with decreasing temperature, although agrees well with existing data at ~1000K.

At temperatures representative of GT operation (<900K), the model is in very good agreement with both low temperature correlations. Moreover, extrapolation of the flow rig data also suggests a high degree of consistency, although lack of

available data at  $\phi = 0.5$  prevents a thorough assessment. Above 900K however, there appears to be less consistency between the low temperature correlations, and to a limited extent, between the flow rig measurements and model predictions. In the first instance, correlation 3 was compiled only for fuel rich conditions and hence is likely to be less valid for lean equivalence ratios. In the second instance, the small difference between the flow rig measurements and model predictions may be the result of the influence of fuel-air mixing delay time on the overall ADT [16].

### NATURAL GAS PREDICTION

Finally, the model was configured for natural gas at 15.8 bar and 848K to establish whether it would predict an auto-ignition failure as witnessed in the test campaign. ADT predictions at the given test conditions are provided for a range of temperatures in Figure 11, with the model clearly demonstrating a ‘no ignition’ event at 850K. Moreover, Figure 12 shows the influence of equivalence ratio on the ADT prediction and substantiates the test observations across almost the entire operating range. According to the model, auto-ignition should have occurred at  $\phi \sim 3.0$  and above, which was evidently not the case. However, given the unknown nature of the boundary layer, the margin of error associated with the mean equivalence ratio measurement may be significant enough to counteract this discrepancy. Furthermore, the maximum duct residence time was derived from the ratio of ADT/detector position and averaged across all operating points, and therefore can only be considered an approximation. Consequently, the duct residence time spread is also given in Figure 12 which clearly shows the possibility of no auto-ignition across the full operating range.

In addition to the model results, Figure 11 also provides predictions from the natural gas correlation (2) and both low temperature methane correlations [12, 13] at the aforementioned operating conditions. Interestingly, the natural gas correlation is almost identical to the model prediction and therefore correctly indicates an auto-ignition failure. However, despite evidence to suggest that natural gas auto-ignites more readily than methane (in this experimental programme as well as in the literature), both low temperature methane correlations incorrectly predict an auto-ignition event at 850K.

### RECOMMENDATIONS

In light of the limited experimental data and the degree of uncertainty associated with the fuel-air mixing characteristics, it is recognised that several improvements could be made to the experimental configuration in order to benefit future studies.

Firstly, it is clear that the maximum temperature range should be extended in order to achieve a robust data set suitable for thorough scientific interrogation. Moreover, the test duct should be lengthened and split into modular sections to provide greater flexibility in operating range as well as providing access for intrusive sampling probes. Intrusive sampling could yield time-averaged measurements of gas composition, pressure and temperature at different axial and radial locations within the test duct. To avoid ignition within probe stagnation/recirculation zones, such measurements would have to be carried out below the auto-ignition temperature of the air-fuel mixture. From these data, steady state profiles of equivalence ratio, velocity and temperature could be obtained and used to validate the

CFD flow rig model. In addition, high frequency response thermocouples could be installed to monitor transient wall temperatures along the test duct and on the fuel injector housing/distributor. Fibre optics could also be used to accurately locate the position of the auto-ignition event within the near-wall region.

A variety of well-characterised fuel injectors could be used to study the effects of fuel-air mixing on ADT. Examples of such are given in [9, 15]. Furthermore, control valves that produce shorter pulse widths should be investigated to improve the accuracy of the second ADT measurement technique. However, due to their reduced flow capacity, it is likely that several valves would need to be installed in parallel.

Fuel preheating should also be improved although control/non-return valve integrity and fuel decomposition problems would need to be addressed.

### CONCLUSIONS

Auto-ignition delay time measurements were successfully obtained for ethylene in a flow rig at representative gas turbine combustor inlet conditions ( $\sim 16$  bar and 850K). Measurements were attempted across a wide range of mean equivalence ratios ( $0.5 < \phi < 3.3$ ) and ADT was thus found to decrease as a function of mean equivalence ratio. Since the test duct measurement range was constrained by geometry, auto-ignition consequently only occurred in very rich fuel-air mixtures: ADT  $\sim 160$  ms at  $\phi \sim 2.6$  and  $\sim 130$  ms at  $\phi \sim 3.3$ . However, since the auto-ignition events were found to occur in the near-wall region, a level of uncertainty must be attributed to both the local equivalence ratio and mixture temperature in light of the CFD results.

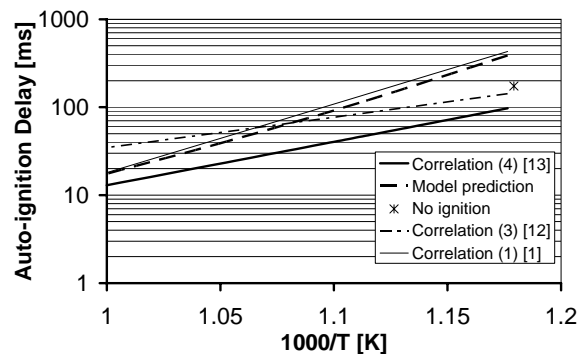


Figure 11: Prediction of natural gas failure to auto-ignite at rig operating limit ( $\phi = 0.5$ )

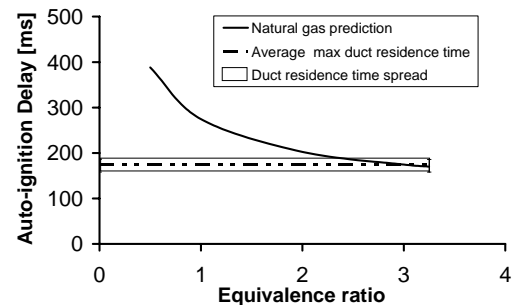


Figure 12: Prediction of natural gas failure to auto-ignite at rig operating limit ( $0.5 < \phi < 3.25$ )



Measurements for methane and natural gas<sup>1</sup> were also attempted across a similar operating range, although no auto-ignition events were recorded. The maximum operating range/residence time of the flow rig was estimated to be ~175ms. As a consequence, it is therefore highly unlikely that current industrial gas turbine engines operating with either methane or natural gas will be exposed to the threat of auto-ignition. It is thus far more likely that the reports of auto-ignition events occurring in the field are, in fact, the result of flashback. Indeed, the fact that auto-ignition was found to occur in the slow moving region near to the duct wall emphasises the importance of boundary layer formation in premix duct design.

Model predictions were found to agree with the ethylene measurements, although improved qualification of the experimental boundary conditions is required in order to better understand the dependence of auto-ignition delay on the physical characteristics of the flow rig.

The chemical kinetic model was compared with existing 'low temperature' measurements and correlations for methane and natural gas at typical GT operating conditions and was found to be in good agreement. Furthermore, the model was also able to predict the failure of natural gas to auto-ignite at the observed test conditions.

## ACKNOWLEDGMENTS

This work was funded by Rolls-Royce, Siemens Industrial Turbines, UK Department of Trade and Industry (DTI) and the European Commission (Fifth Framework Programmes: PRECCINSTA, Contract No. ENK5-CT-2000-00060 and AFTUR, Contract No. ENK5-CT-2002-00662).

## REFERENCES

1. "Ignition delay characteristics of methane fuels", L. J. Spadaccini, M. B. Colket III, *Progress in Energy Combustion Science*, 20:431-460, 1994.
2. ADT data for hydrogen, ethylene and propane, J. Shepherd. [<http://www.galcit.caltech.edu/EDL/public/resources.html>]
3. "Shock-tube study of methane ignition under engine-relevant conditions: experiments and modelling", J. Huang et al, *Combustion and Flame*, 136:25 – 42, 2004.
4. "Shock-tube investigation of comparative ignition delay times for C1-C5 alkanes", A. Burcat, K. Scheller, A. Lifshitz, *Combustion & Flame* 16: 29 – 33, 1971.
5. "Effects of propane on ignition of methane-ethane-air mixtures", C. K. Westbrook, W. J. Pitz, *Comb. Sci. Tech.*, 33: 315-319, 1983.
6. "A shock-tube investigation of the ignition of lean methane and n-butane mixtures with oxygen", R. M. R. Higgin, A. Williams, 12<sup>th</sup> Symposium (International) on Combustion, p 579, 1969.
7. "Shock tube investigation of ignition in methane-oxygen-argon mixtures", Lifshitz et al, *Combustion & Flame* 16: 311 – 321, 1971.
8. "Shock-initiated ignition methane-propane mixtures", M. Frenlach, D. E. Bornside, *Combustion & Flame* 56: 1 – 27, 1984.

9. "Spontaneous ignition delay characteristics of hydrocarbon fuel-air mixtures", A. Lefebvre, W. Freeman, L. Cowell, NASA Contractor Report 175064, 1986.
10. "Influence of pressure on auto-ignition characteristic of gaseous hydrocarbon-air mixtures", L. H. Cowell, A. H. Lefebvre, SAE paper 860068, 1986.
11. "Spontaneous Ignition Delay Characteristics of Gaseous Hydrocarbon-Air Mixtures", G. Freeman, A. Lefebvre, L. H. Cowell, *Combustion and Flame*, 58: 153-162, 1984.
12. "Ignition delay times of ram accelerator CH<sub>4</sub>/O<sub>2</sub>/diluent mixtures", E. L. Petersen, D. F. Davidson, R. K. Hanson, *Journal of Propulsion and Power*, Vol 15, No. 1, pp. 82-91, Jan 1999.
13. "Reaction mechanisms for methane ignition", S. C. Li, F. A. Williams, ASME Paper No. 2000-GT-145, Munich, Germany, May 8-11, 2000.
14. "The oxidation of methane at elevated pressures: Experiments and Modeling", T. B. Hunter, H. Wang, T. A. Litzinger, M. Frenklach, *Combustion and Flame*, 97:201 – 224, 1994.
15. "Correlation of ignition delay with fuel composition and state for application to gas turbine combustion", S. Samuelsen et al, Contract No. 00-01-SR084CS UCI Final Report, January 2003. [<http://www.clemson.edu/scies/00-01-SR084.pdf>]
16. "Autoignition characteristics of gaseous fuels at representative gas turbine conditions", C. J. Goy et al, ASME Paper No. 2001-GT-0051, New Orleans, USA, June 4-7, 2001.
17. "The auto-ignition of propane at intermediate temperatures and pressures", P. Cadman, G. O. Thomas, P. Butler, *Physical Chemistry Chemical Physics*, 2:5411 – 5419, 20.
18. "Autoignition Delay Time Measurements of Ruhr Natural Gas in a High Pressure Flowing Rig", G-J. Sims, R. W. Copplestone, M. I. Wedlock, Report No. QINETIQ/FST/CR041853; undertaken as part of the PRECCINSTA Fifth Framework Programme, Contract No. ENK5-CT-2000-00060.
19. "Numerical Study of the Turbulent Flow Past an Airfoil with Trailing Edge Separation", C M Rhie, W L Chow, *AIAA Journal* 31, 1525–1533 (1983)
20. "Towards the Ultimate Conservative Differencing Scheme II: Monotonicity and Conservation Combined in a Second Order Scheme", B van Leer, *Journal of Computational Physics* 14, 361 (1974)
21. "Detailed reaction mechanism for small hydrocarbons combustion", A. A. Konnov, Release 0.4. [<http://homepages.vub.ac.be/~akonnov/1998>]
22. [[http://www.me.berkeley.edu/gri\\_mech/version30/text30.html#targets](http://www.me.berkeley.edu/gri_mech/version30/text30.html#targets)].
23. Private communication with author, August 14<sup>th</sup>, 2000.
24. CHEMKIN Collection, R.J. Kee et al, Release 3.6, Reaction Design, Inc, San Diego, CA (2000).

<sup>1</sup> based on the German Ruhr gas field supply